Independent Reproduction of the Bell-Triplet Spin-Readout Notes

May 13, 2026

Abstract

This note reproduces the essential numerical claims in `docs/internal_note/main.pdf` and `docs/internal_note/risk_audit.pdf` from raw PIKOE tables, PIKOE outlists, Saclay-amplitude CSV grids, and the saved risk-sweep JSON outputs. No original source files were modified. The new code, plots, and tables live in `src/gpt-claude-reproduction/`.

1 Scope and Provenance

The reproduction uses the PWA93, AV18, and AV8' Saclay CSV files for the elementary pp amplitude, the PIKOE sample tables for $^{7}\mathrm{Li}(p,2p)^{6}\mathrm{He}$ and $^{17}\mathrm{F}(p,2p)^{16}\mathrm{O}$, and the risk-audit JSON files for the already-run A2/A3/B1/D5 sweeps. All Bell-readout quantities below were recomputed in the new script `src/gpt-claude-reproduction/reproduce_results.py`; generated tables are in `src/gpt-claude-reproduction/tables/`.

At the free-pp target point the reproduction gives $S(151\,\mathrm{MeV}, 90^\circ) = 0.9943$ and $d\sigma/d\Omega = 3.72$ mb/sr using PWA93 with Coulomb added. The production path is therefore a PWA93-based reproduction of the note's results; it is not a fresh chiral-EFT amplitude calculation.

2 Free pp Bell Window

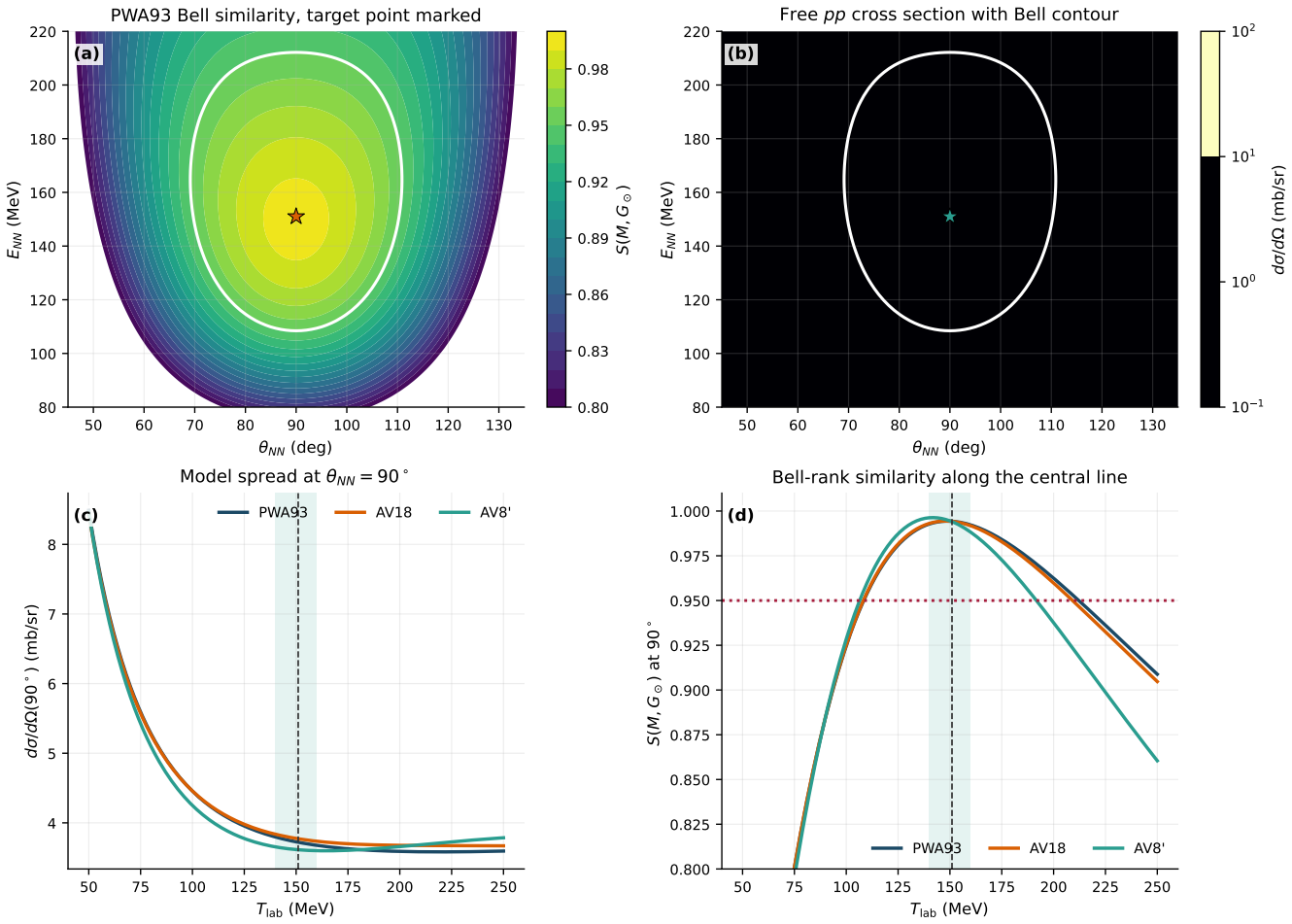

Figure 1: Independent reconstruction of the elementary pp Bell-window structure. The PWA93 similarity island contains the intended $(E_{NN}, \theta_{NN}) = (151\,\text{MeV}, 90^\circ)$ point; AV18 and AV8' track PWA93 closely near the central line but are used here as model-spread checks rather than as chiral truncation errors.

3 Production Scans

Table 1: Beam-energy scan reproduced from the PIKOE tables and outlists. Stars mark the beam energies used for the production forecasts.

Target	E_{beam} MeV/u	BW frac %	$\langle E_{NN} \rangle$ MeV	$\langle \theta_{NN} \rangle$ deg	$\langle S \rangle$	σ_{BW} μb
^{7}Li	100	35.4	136.3	78.9	0.9737	4.49
^{7}Li	110	59.9	137.5	83.8	0.9782	13.06
^{7}Li	120	51.6	152.4	80.5	0.9715	9.25
^{7}Li	130*	76.0	148.0	83.9	0.9825	34.04
^{7}Li	140	48.9	154.1	83.1	0.9679	13.26
^{7}Li	151	42.5	150.1	84.9	0.9742	15.00
^{7}Li	160	58.4	157.1	83.0	0.9812	35.53
^{7}Li	170	44.0	157.8	83.2	0.9737	18.97
^{7}Li	180	26.6	137.4	88.6	0.9855	10.74
^{7}Li	195	28.2	138.3	88.1	0.9851	11.32
^{17}F	100	28.1	151.6	83.8	0.9734	11.98
^{17}F	110	28.0	156.6	84.0	0.9750	13.83
^{17}F	120	36.7	152.5	86.9	0.9778	22.81
^{17}F	130	30.0	156.3	86.4	0.9700	17.08
^{17}F	140*	45.0	156.6	86.6	0.9786	33.34
^{17}F	151	34.2	153.8	87.8	0.9780	24.14
^{17}F	160	35.4	154.6	87.7	0.9742	23.88
^{17}F	170	23.3	136.8	92.6	0.9861	15.21
^{17}F	180	25.0	138.3	91.8	0.9859	15.71
^{17}F	195	26.1	144.2	89.6	0.9883	15.28

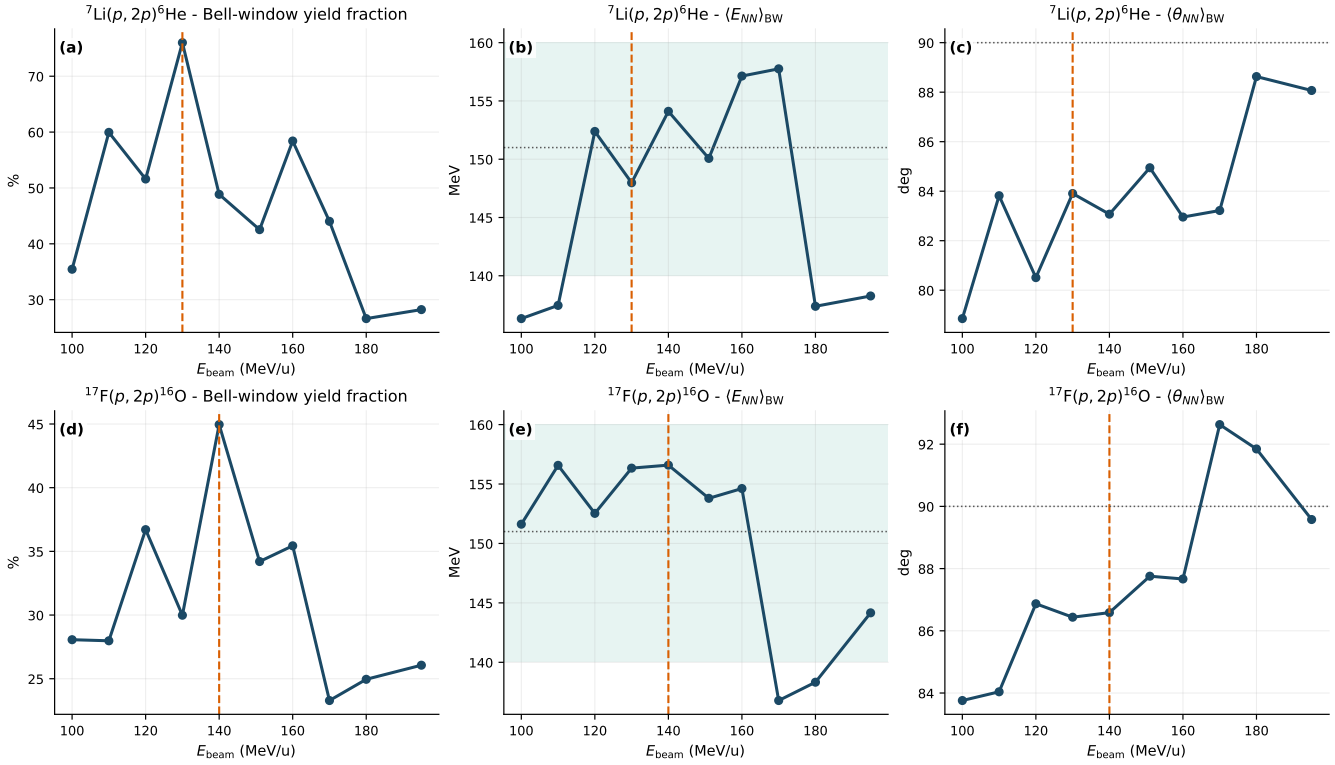

Figure 2: Beam-energy scan diagnostics. The reproduced optima are 130 MeV/u for ^{7}Li and 140 MeV/u for ^{17}F, matching the internal note.

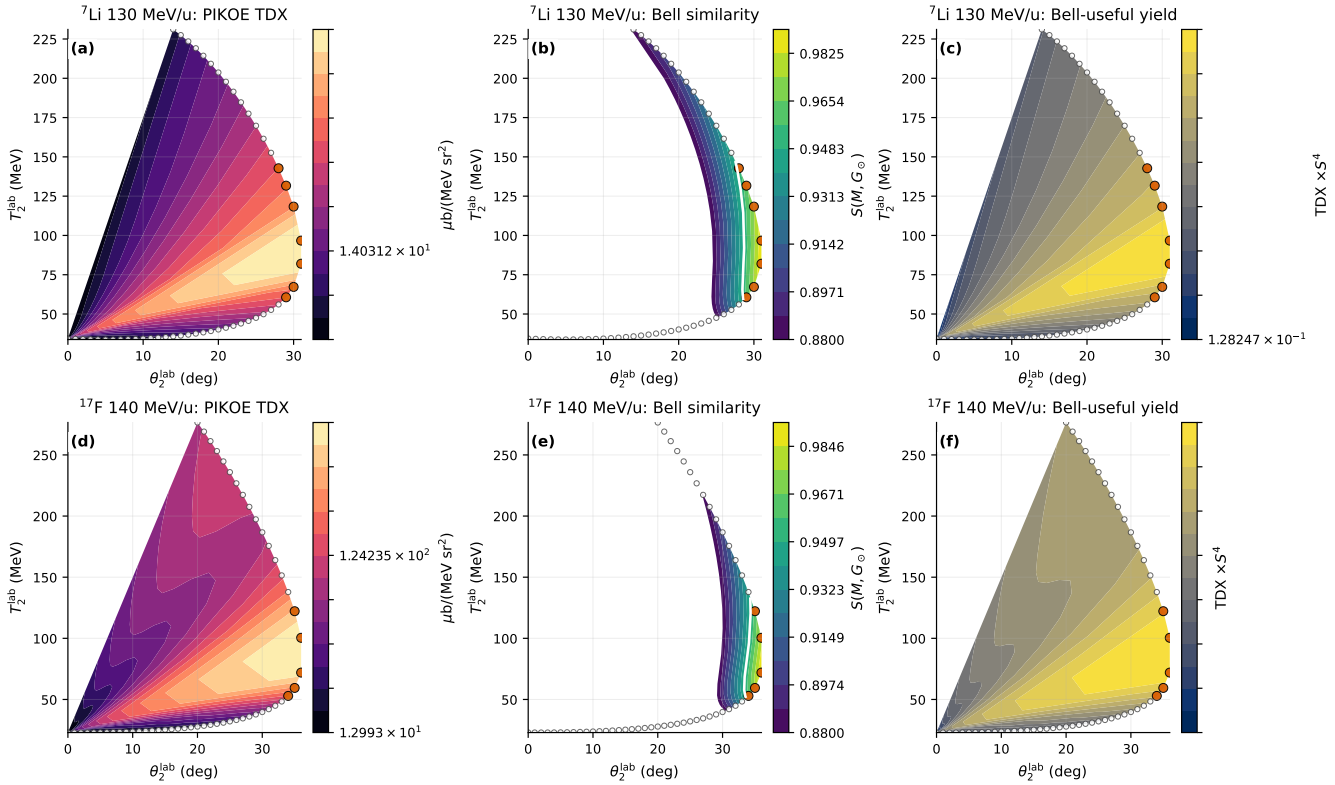

Figure 3: Phase-space yield maps at the production energies. Orange points are bins with $S(M, G_\odot) \geq 0.95$. The right column weights the PIKOE TDX by a high power of the Bell similarity to make the useful kinematic ridge visually explicit.

4 Bell Readout and Counting

Table 2: Scenario forecasts using the absolute-precision definition $\sigma(s_b^z) = 0.05$. The realistic rows reproduce the headline values: ^{7}Li gives $A_z = 0.130$, $\dot{N} = 238$ s^{-1}, $t_{5\%} = 42$ s; ^{17}F gives $A_z = 0.030$, $\dot{N} = 2.33 \times 10^{-2}$ s^{-1}, $t_{5\%} = 119$ h.

Target	Scenario	P_T	P_b	A_z	$\dot{N}$ (s^{-1})	$t_{5\%}$
^{7}Li	Conservative	0.15	0.50	0.075	51.1	5.8 min
^{7}Li	Realistic	0.20	0.65	0.130	238	42.0 s
^{7}Li	Optimistic	0.30	0.85	0.255	2.38e+03	1.9 s
^{17}F	Conservative	0.15	0.10	0.015	0.005	41.1 d
^{17}F	Realistic	0.20	0.15	0.030	0.0233	5.0 d
^{17}F	Optimistic	0.30	0.20	0.060	0.07	17.6 h

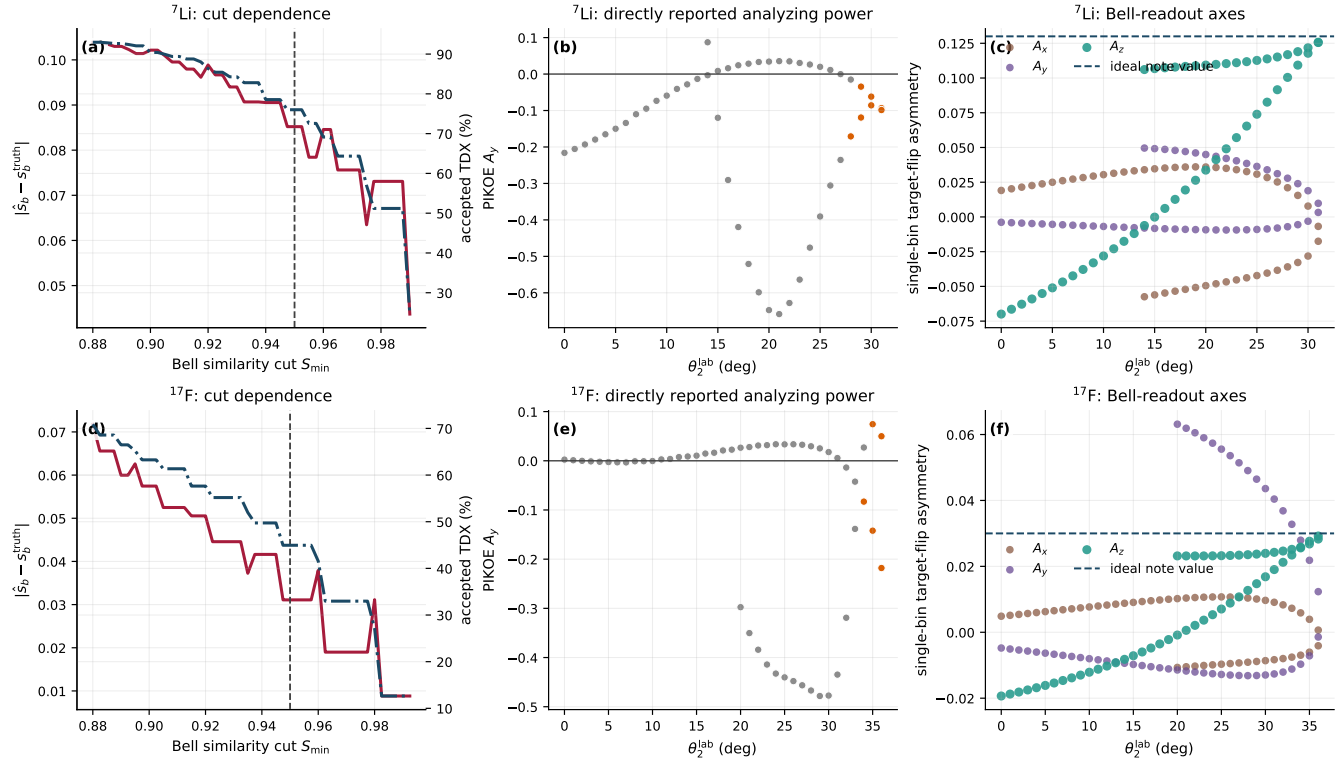

Figure 4: Readout diagnostics at the production energies. The full-amplitude physical readout gives $A_z = 0.1231$ for ^{7}Li and $A_z = 0.0280$ for ^{17}F at the $S_{\min} = 0.95$ cut, while the ideal Bell-limit scenario table uses $P_T P_b = 0.130$ and 0.030.

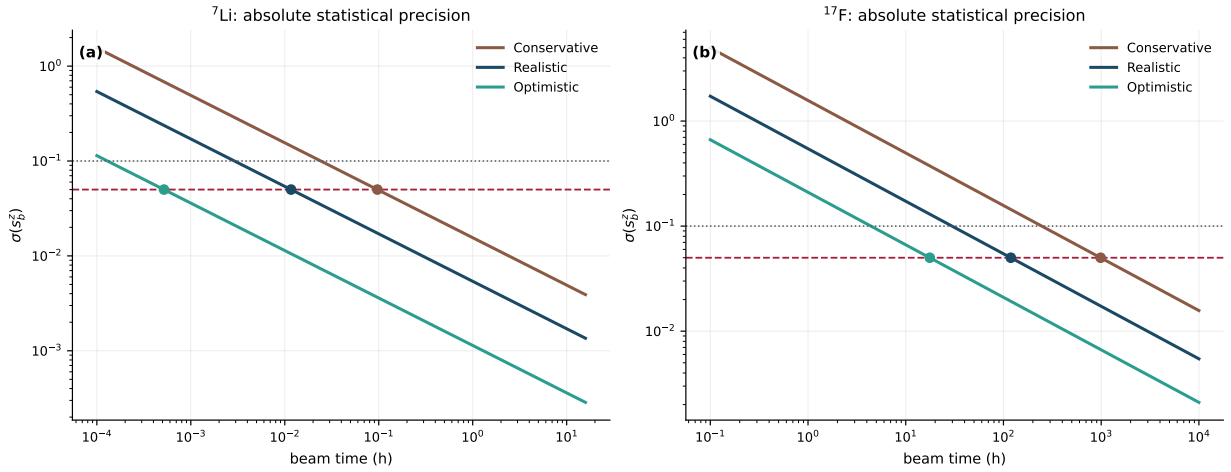

Figure 5: Absolute statistical precision versus beam time for the conservative, realistic, and optimistic scenarios.

5 Systematics and Risk Audit

Table 3: Risk-axis ranges reproduced from the saved JSON sweeps. A1 is the active-proton spin-density band; A2, A3, B1, and D5 are the production pipeline sweeps.

Target	Axis	Min A_z	Max A_z	Baseline	Full spread / baseline
^{7}Li	A1_sigma_z	0.09750	0.12350	0.13000	20.00%
^{7}Li	A2	0.12296	0.12314	0.12306	0.14%
^{7}Li	B1	0.12299	0.12313	0.12312	0.11%
^{7}Li	D5	0.12306	0.12306	0.12306	0.00%
^{7}Li	A3	0.12303	0.12309	0.12306	0.05%
^{17}F	A1_sigma_z	0.02790	0.03000	0.03000	7.00%
^{17}F	A2	0.02795	0.02797	0.02796	0.07%
^{17}F	B1	0.02793	0.02800	0.02794	0.24%
^{17}F	D5	0.02785	0.02798	0.02796	0.44%
^{17}F	A3	0.02795	0.02797	0.02796	0.06%

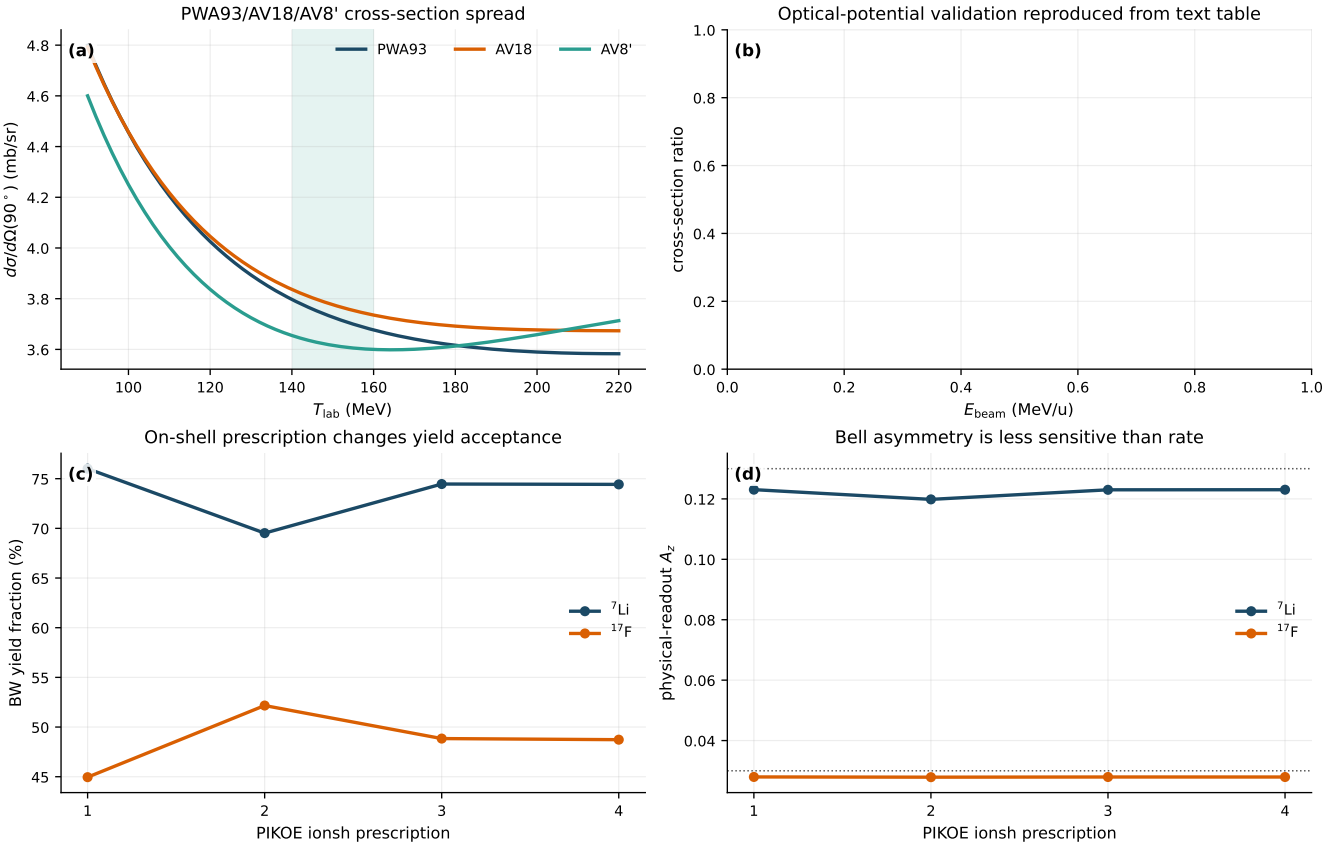

Figure 6: Model and internal PIKOE systematics. The on-shell prescription and optical-potential checks mostly move rates; the Bell-readout asymmetry is much less sensitive.

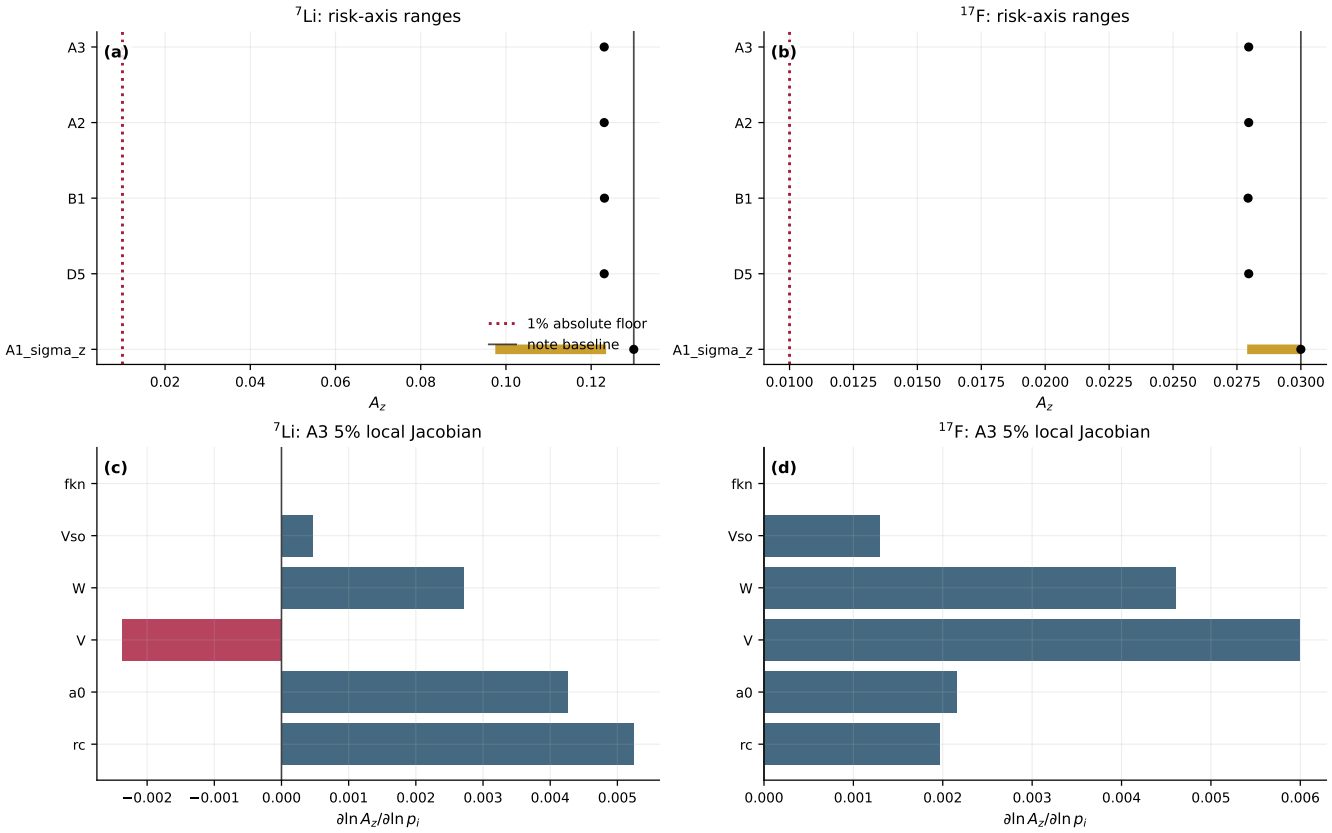

Figure 7: Risk-audit reproduction. The dominant horizontal range is the A1 $\langle \sigma_z \rangle$ band; A2/A3/B1/D5 are sub-percent in the saved production sweeps. The lower panels reproduce the small A3 logarithmic Jacobians.

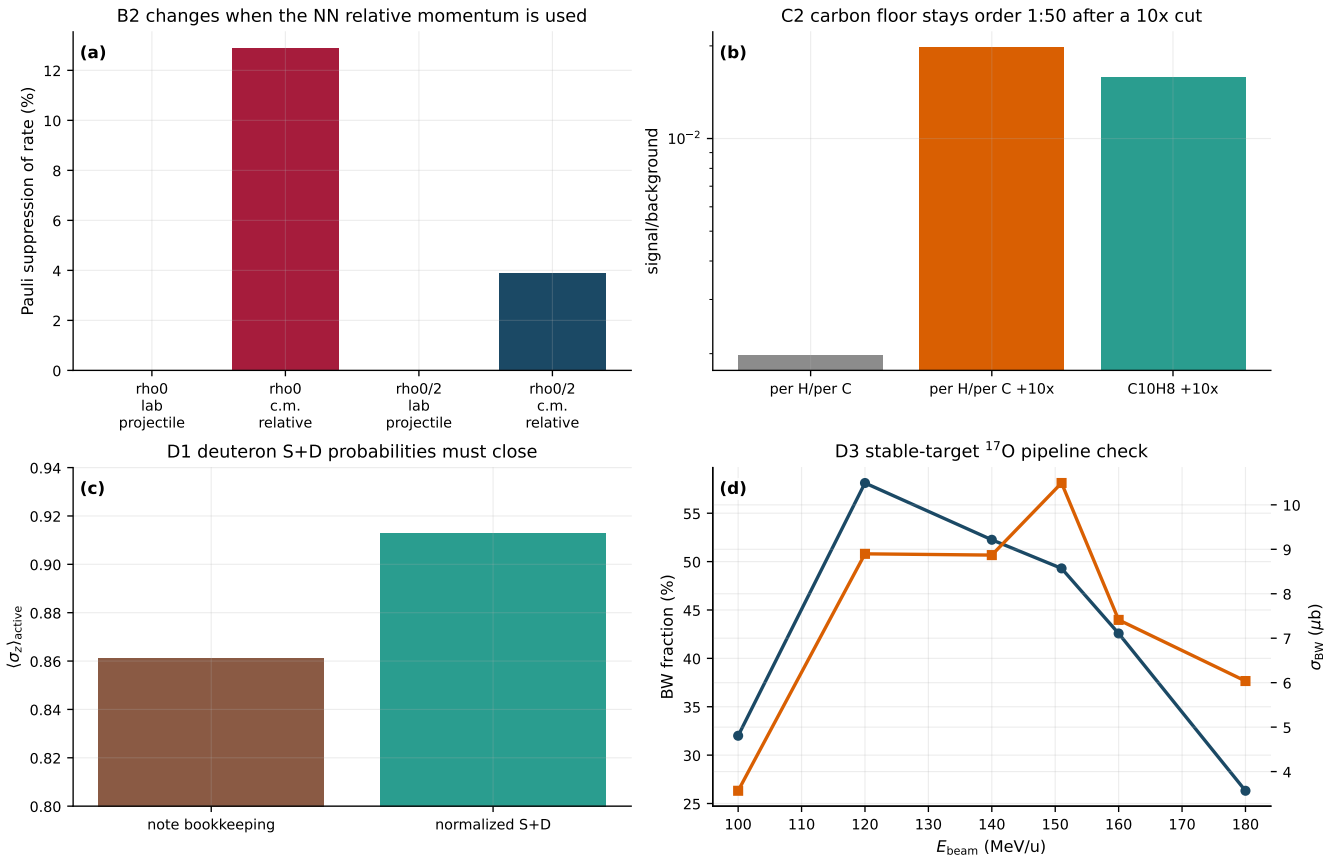

Figure 8: Bookkeeping and cross-check reproductions. The Pauli-blocking panel shows why the momentum convention matters; the carbon panel keeps the order-of-magnitude S/B floor visible; the deuteron panel shows the effect of closing the $S + D$ probability; and the last panel reproduces the ^{17}O pipeline check.

6 Mistake-Oriented Findings

Topic	Reproduction finding
Frame handling	The reproduced BW bins are not exactly in a common lab spin frame: ^{7}Li has weighted $\theta(\mathbf{k}_i, -\hat{z}) = 7.73^\circ$ and ^{17}F has 6.15°. This is small enough to look like a few-percent effect in the weighted F_{zz} factor, but it is not the zero-rotation assumption stated in the prose.
Pauli blocking	Using the lab projectile momentum gives $Q = 0.99986$ at ρ_0; using the NN c.m. relative momentum gives $Q = 0.871$. The old "$< 0.01\%$" statement is a lab-momentum result, not the relative-momentum result.
Amplitude source	The production runs reproduce PWA93-based Saclay amplitudes. AV18/AV8' are useful spread checks, but this package found no production use of a live chiral-EFT amplitude path.
$t_{5\%}$ definition	The scenario table above uses the main-note absolute definition $\sigma(s_b^z) = 0.05$. The risk addendum also uses a relative definition that scales as $(P_b\langle\sigma_z\rangle)^{-2}$. These are different observables and should not share one label.
^{17}F significance	The realistic ^{17}F forecast remains $A_z = 0.030$, below the addendum's $A_z \geq 0.05$ discovery threshold. It is a feasible signal estimate, not a discovery-significance case under that threshold.
Carbon floor	The reproduced arithmetic gives $S/B \simeq 0.002$ raw and about 0.02 after a $10\times$ BW rejection, not 0.2–0.5.
Deuteron calibration	The note bookkeeping values $P_S = 0.89$ and $P_D = 0.058$ sum to 0.948. Closing $P_S + P_D = 1$ shifts $\langle\sigma_z\rangle_{\text{active}}$ from 0.861 to 0.913.
^{7}Li valence wording	The alpha-core p-shell picture is one valence proton plus two valence neutrons, not three valence protons plus four valence neutrons in the $1p$ shell.

7 Artifacts

The code is `src/gpt-claude-reproduction/reproduce_results.py`. The canonical machine-readable outputs are `src/gpt-claude-reproduction/data/summary.json` and the CSV/TEX tables under `src/gpt-claude-reproduction/tables/`. The figure PDFs and PNGs are under `src/gpt-claude-reproduction/figures/`.